GSA DATA REPOSITORY 2016261

Control of lithospheric inheritance on neotectonic activity in northwestern Canada?

Pascal Audet, Christian Sole, and Andrew J. Schaeffer

Department of Earth and Environmental Sciences, University of Ottawa, Ottawa, Canada, K1N 6N5

TELESEISMIC SHEAR-WAVE SPLITTING ANALYSIS

Upon entering an anisotropic medium characterized by azimuthal anisotropy, upgoing radially-polarized and planar SKS waves will split into two orthogonal components, one of which will travel along the fast axis of seismic propagation (with azimuth ϕ), whereas the other component will travel along the perpendicular slow axis. Depending on the thickness of the medium and wave speed difference between the fast and slow axis of hexagonal symmetry, a delay time δt will accumulate between the two polarized shear waves. The splitting process is thus completely characterized by the parameters ϕ and δt (Silver, 1996). Incidentally, shear waves initially travelling along one of the symmetry axes will not produce any observable splitting. These results are called "null" measurements and can further help to constrain the orientation ϕ. Anisotropy that varies with depth or described by a different class of symmetry (or hexagonal anisotropy with a dipping axis of symmetry) will give rise to more complicated patterns of splitting.

We used 6 stations from the Transportable Array of USArray (TA), 5 stations from the Yukon-Northwest Seismograph Network (NY), and one station from the Polaris Network (PO)

(Table DR1). We selected waveforms for all magnitude M>6.0 events with signal-to-noise ratio greater than 4 dB in the epicentral distance range of 85-140° that occurred between April 2014 and March 2016. Waveforms are rotated into a longitudinal-radial-tangential (LQT) coordinate system and filtered using a 0.05-0.15 Hz band-pass filter (Currie et al., 2004). Shear wave splitting analysis at each station was carried out using the SplitLab software (Wüstefeld et al., 2008) and resulted in 61 successful (i.e. non-null, see below) splitting measurements from SKS phases (Tables DR1 and DR2). The number of estimates is low for recently installed stations of the TA network. SplitLab performs the splitting analysis based on two distinct methods. The energy minimization method (also called SC method) (Silver and Chan, 1991) seeks the splitting parameters ϕ and δt for which the energy of the transverse shear wave component is minimized after inverting the splitting process. In contrast, the rotation-correlation method (also called the RC method) rotates the seismogram of interest into a test coordinate frame and searches for the pair of splitting parameters that gives the maximum cross correlation between the transverse and radial SKS components (Wüstefeld et al., 2008).

Results are first classified into nulls if they satisfy two criteria: 1) SNR of the tangential component of the SKS phase is below 3 dB, or 2) the difference in ϕ obtained from the SC and RC methods is between 22 and 68 degrees (Wüstefeld and Bokelmann, 2007). Both nulls and non-nulls are then qualitatively evaluated in terms of "Good", "Fair" and "Poor" results based on the ratio of RC and SC delay times ($\rho = \delta t_{RC}/\delta t_{S}$) and the difference between RC and SC azimuths ($\delta\phi = \max[|\phi_{RC}-\phi_{SC}|, |\phi_{SC}-\phi_{RC}|]$) (Wüstefeld and Bokelmann, 2007). For Nulls, these correspond to $\rho < 0.2$, $37° < \delta\phi < 53°$ for “Good” measurements; $\rho < 0.3$, $32° < \delta\phi < 58°$ for “Fair”; and “Poor” otherwise. For non-Nulls, these correspond to $0.8 < \rho < 1.1$, $\delta\phi < 8°$ for

“Good” measurements; $0.7 < \rho < 1.2$, $\delta\phi < 15°$ for “Fair”; and “Poor” otherwise. Parameter uncertainty was estimated from the 95% confidence interval using an F-test (Walsh et al., 2013).

An example result of parameter estimation for a single event recorded at station EPYK is shown in Figure DR1. Figure DR2 shows the compilation of "good" and "fair", non-null results for station EPYK, sorted by back-azimuth of incoming SKS waves. These results show tightly clustered estimates of both ϕ and δt, and we interpret these in terms of a single layer with horizontal anisotropy. We note, however, that the event distribution is not uniform in back-azimuth, and the single-layer assumption may not hold in reality. We then separately perform a vector average of all "good" and "fair" non-null results (weighting the estimates equally) for both the SC and RC techniques, and obtain final estimates by vector averaging the results of both techniques into a single estimate of ϕ and δt for each station (Table DR1), further preventing us from considering more complex (i.e., multi-layered or dipping) anisotropy models. We also ignore covariance and our error estimates are likely lower bounds. Figure DR3A shows all ‘fair’ and ‘good’ measurements at each station.

Null estimates can also provide qualitative information on the robustness of the splitting parameters. Null measurements occur because: 1) there is no detectable anisotropy beneath the station; or 2) the incoming SKS wave propagates along either the slow or fast axis of anisotropy. We plot the back-azimuth of all “good” null measurements as rose diagrams in Figure DR3B, along with the estimated splitting parameters (reproduced from Figure 1B). Each set of measurements is binned in 10° back-azimuth and the length of the bars is proportional to the percent number of measurements in each bin. These results show that the dominant back-azimuths of “null” measurements are aligned with either the fast axis or perpendicular to it, thus qualitatively confirming that the splitting measurements are robust.

NOTES

The SplitLab software used in this study was translated from Matlab® to Python and thoroughly tested against published results. The Python software makes extensive use of the ObsPy module developed by Beyreuther et al. (2010), and is available upon request.

REFERENCES CITED

Beyreuther, R. Barsch, L. Krischer, T. Megies, Y. Behr and J. Wassermann, 2010, ObsPy: A Python Toolbox for Seismology: Seism. Res. Lett., v. 81, no. 3, p. 530-533.

Currie, C. A., Cassidy, J. F., Hyndman, R. D., and Bostock, M. G., 2004, Shear wave anisotropy beneath the Cascadia subduction zone and western North American Craton: Geophys. J. Int., v. 157, p. 341–353.

Silver, P. G., 1996, Seismic anisotropy beneath the continents: Probing the depths of geology: Annu. Rev. Earth Planet. Sci., v. 24, p. 385-432.

Silver, P. G., and Chan, W. W., 1991, Shear-wave splitting and subcontinental mantle deformation: J. Geophys. Res., v. 96, p. 429-454.

Walsh, E., Arnold, R., and Savage, M. K., 2013, Silver and Chan revisited: J. Geophys. Res., v. 118, p. 5500-5515.

Wüstefeld, A., and Bokelmann, G., 2007, Null detection in shear-wave splitting measurements: Bull. Seism. Soc. Am., v. 97, no. 4, p. 1204-1211.

Wüstefeld, A., Bokelmann, G., Zaroli, C., and Barruol, G., SplitLab: A shear-wave splitting environment in Matlab: Comp. Geosci.

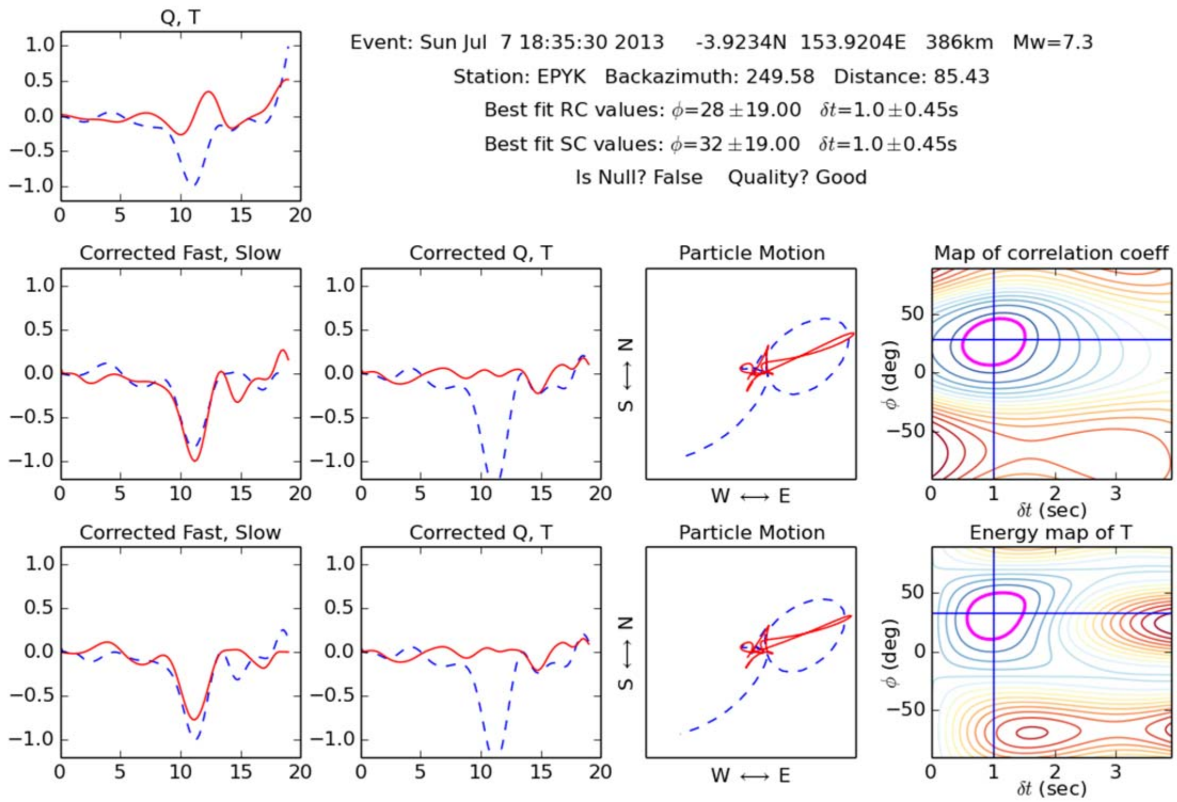

Figure DR1. Example result of a single-event estimate of SKS splitting obtained at station EPYK. The text describes the earthquake parameters and best-fit estimates for both the RC and SC techniques, as well as the quality factor. The top left panel shows the longitudinal (Q, blue) and tangential (T, red) seismograms for a hand picked window around the predicted SKS phase arrival. The bottom two rows of panels show inversion results for the RC (middle row) and SC (bottom row) techniques. For each technique, the first two panels represent the fast (blue) and slow (red) components and the longitudinal (blue) and tangential (red) components after removing the effect of splitting. Horizontal axis is time in seconds. The last two panels show the initial (blue) and corrected (red) particle motion in the horizontal plane, and the misfit contours (low misfit in blue, high misfit in red), shown either as a map of the correlation coefficient between the corrected fast and slow components (RC) or the energy of the tangential component after correction. The magenta contours show the 95% confidence interval.

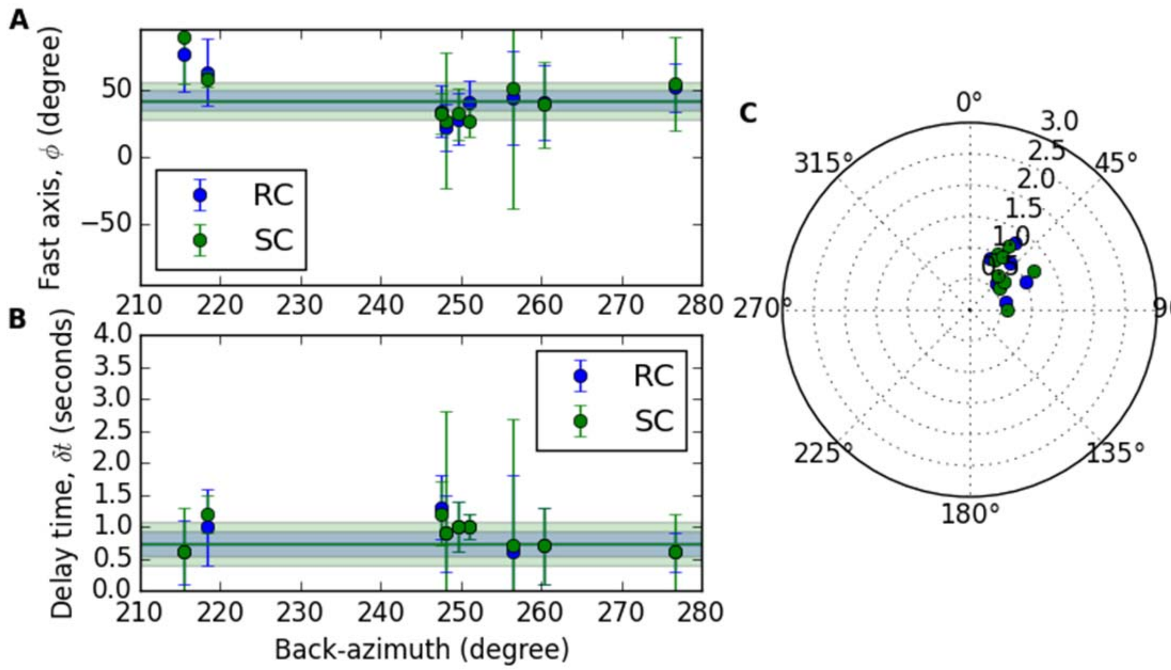

Figure DR2. Compilation of SKS splitting results for all “Good” and “Fair” non-nulls for station EPYK. **A**: Azimuth of fast shear-wave propagation; **B**: Delay time between fast and slow shear waves. Blue and Green symbols represent results obtained from the RC and SC techniques, respectively. The blue and green shaded areas show the standard deviation of each quantity around the mean value (solid lines) obtained from a vector average of individual measurements. **C**: Representation of the estimated azimuths and delay times as a polar plot with delay time increasing radially from the origin, which emphasizes the clustering of splitting parameters.

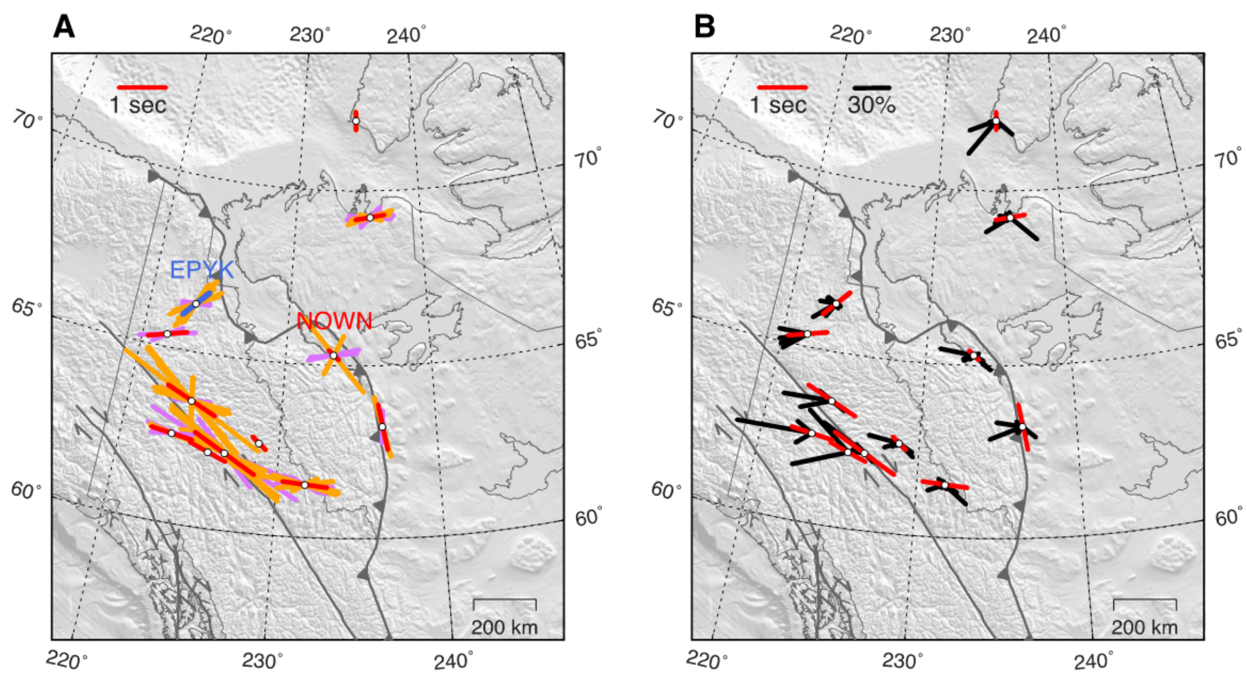

Figure DR3. **A**. Map of SKS splitting results for all “fair” and “good” non-nulls shown as purple and orange bars, respectively. Except for station NOWN that displays variable fast axis directions perhaps indicative of multi-layered anisotropy, all stations show a tight distribution around the average parameters shown in red. Station EPYK is highlighted in blue. **B**. Map of null measurements for all “good” nulls plotted as rose diagrams (black bars) of back-azimuths of incoming SKS waves. The bars represent the percent number of events per 10° back-azimuth bin. Estimated SKS splits appear in red (reproduced from Figure 1B) in both **A** and **B**.

Table DR1: Station average splitting parameters

Stations				RC Avg.				SC Avg.					Station Avg.			
Network	Name	Lon (°)	Lat (°)	ϕ (°)	σ_ϕ	δt (s)	$\sigma_{\delta t}$	ϕ (°)	σ_ϕ	δt (s)	$\sigma_{\delta t}$	#	ϕ (°)	σ_ϕ	δt (s)	$\sigma_{\delta t}$
TA	M31M	-134.391	62.202	-74.00	29.00	0.80	0.80	-64.00	37.00	0.90	1.00	1	-69.00	33.00	0.85	0.90
NY	MMPY	-131.262	62.619	-52.00	15.00	0.40	0.20	-48.00	41.00	0.40	0.90	1	-50.00	28.00	0.40	0.55
PO	NOWN	-126.715	65.294	-49.21	32.27	0.26	0.76	-47.09	32.64	0.35	0.73	3	-48.15	32.45	0.30	0.74
TA	I29M	-138.306	63.361	69.85	45.72	0.69	1.02	78.20	22.73	1.00	0.65	2	74.02	34.22	0.84	0.83
TA	A36M	-125.250	71.990	0.00	19.00	0.40	0.20	-1.00	38.00	0.40	0.60	1	-0.50	28.50	0.40	0.40
TA	C36M	-124.070	69.347	83.77	11.36	0.61	0.25	78.40	17.63	0.65	0.52	7	81.08	14.49	0.63	0.38
NY	WGLY	-123.458	63.228	-13.25	19.24	1.00	0.43	-8.12	20.94	0.96	0.46	2	-10.69	20.09	0.98	0.45
TA	M30M	-136.793	62.576	-77.44	45.21	0.90	1.02	-87.04	17.72	0.91	0.41	2	-82.24	31.47	0.90	0.72
NY	FARO	-133.348	62.230	-63.34	20.81	1.46	0.48	-59.07	12.86	1.60	0.41	9	-61.21	16.84	1.53	0.44
NY	MAYO	-135.892	63.596	-66.42	10.46	1.15	0.25	-64.26	14.26	1.23	0.35	14	-65.34	12.36	1.19	0.30
TA	EPYK	-136.719	66.370	41.96	7.91	0.74	0.20	41.52	13.49	0.73	0.34	9	41.74	10.70	0.73	0.27
NY	TGTN	-128.273	61.527	-84.05	10.83	0.95	0.19	-85.16	8.76	0.98	0.26	10	-84.61	9.80	0.96	0.22

Table DR2: Individual Station Splitting Parameters

	Event Info					RC				SC			
Station	Date	Lon (°)	Lat (°)	Mag	Φ (°)	ϕ (°)	σ_ϕ	δt (s)	$\sigma_{\delta t}$	ϕ (°)	σ_ϕ	δt (s)	$\sigma_{\delta t}$
A36M	8/24/14	-73.57	-14.60	6.8	130.4	0.00	19.00	0.40	0.20	-1.00	38.00	0.40	0.60
	5/24/15	-175.96	-19.39	6.2	-131.6	76.00	37.00	0.90	0.70	72.00	10.00	1.00	0.30
	4/17/15	-178.60	-15.88	6.5	-128.2	-85.00	33.00	0.90	0.70	85.00	32.00	1.00	0.80
	4/7/15	-173.22	-15.17	6.3	-133.0	84.00	19.00	0.80	0.40	83.00	28.00	0.80	0.50
C36M	11/26/14	126.58	1.96	6.8	-71.1	57.00	17.00	0.50	0.30	44.00	44.00	0.60	1.90
	5/21/14	88.04	18.20	6.0	-30.3	-73.00	33.00	0.50	0.70	-75.00	89.00	0.50	2.00
	5/15/14	122.06	9.38	6.3	-64.4	72.00	10.00	0.60	0.20	80.00	44.00	0.60	1.90
	11/23/13	-176.54	-17.12	6.5	-130.5	-88.00	45.00	0.60	1.10	78.00	39.00	0.70	1.00
	9/16/15	151.48	-6.01	6.1	-108.9	41.00	16.00	1.00	0.20	26.00	11.00	1.00	0.20
	12/7/14	154.46	-6.51	6.6	-111.9	22.00	17.00	0.90	0.60	27.00	51.00	0.90	1.90
	11/21/14	127.06	2.30	6.5	-83.3	52.00	18.00	0.60	0.30	54.00	35.00	0.60	0.60
	11/1/14	-177.76	-19.69	7.1	-141.7	63.00	25.00	1.00	0.60	58.00	6.00	1.20	0.30
EPYK	7/29/14	146.77	-3.42	6.0	-103.6	44.00	35.00	0.60	1.20	51.00	89.00	0.70	2.00
	5/7/14	154.90	-6.96	6.0	-112.5	34.00	19.00	1.30	0.50	32.00	15.00	1.20	0.50
	8/1/13	-173.50	-15.24	6.0	-144.5	77.00	29.00	0.60	0.50	89.00	35.00	0.60	0.70
	7/7/13	153.92	-3.92	7.3	-110.4	28.00	19.00	1.00	0.40	32.00	19.00	1.00	0.40
	4/16/13	142.54	-3.22	6.6	-99.7	40.00	28.00	0.70	0.60	39.00	32.00	0.70	0.60
	9/16/15	151.48	-6.01	6.1	-105.8	-57.00	89.00	0.40	2.00	-66.00	89.00	0.40	2.00

continued on next page

FARO

continued from previous page

	Event Info					RC				SC			
Station	Date	Lon (°)	Lat (°)	Mag	Φ (°)	ϕ (°)	σ_ϕ	δt (s)	$\sigma_{\delta t}$	ϕ (°)	σ_ϕ	δt (s)	$\sigma_{\delta t}$
	5/22/15	163.22	-11.11	6.8	-118.4	-55.00	13.00	3.00	0.70	-58.00	9.00	2.90	0.90
	5/22/15	163.70	-11.06	6.9	-118.9	-75.00	20.00	3.50	0.90	-64.00	13.00	3.60	0.80
	2/27/15	122.53	-7.30	7.0	-80.7	-45.00	31.00	0.70	0.90	-51.00	36.00	0.80	0.80
	11/15/14	126.52	1.89	7.1	-80.0	-53.00	89.00	1.10	2.00	-53.00	30.00	1.10	0.90
	11/1/14	-177.76	-19.69	7.1	-138.7	-71.00	30.00	1.70	1.10	-65.00	6.00	1.90	0.50
	10/9/14	-110.81	-32.11	7.0	160.9	-54.00	89.00	1.50	2.00	-44.00	27.00	1.80	1.40
	7/14/14	126.48	5.71	6.3	-78.2	-40.00	31.00	0.40	0.60	-37.00	47.00	0.40	1.90
	5/4/14	179.09	-24.61	6.6	-137.6	-74.00	89.00	1.90	1.80	-68.00	8.00	2.10	0.80
I29M	2/15/16	-175.48	-21.00	6.0	-145.6	81.00	21.00	0.80	0.40	80.00	29.00	0.80	0.50
	1/11/16	126.86	3.90	6.5	-83.9	57.00	89.00	0.70	2.00	77.00	35.00	1.20	1.20
M30M	4/13/16	94.90	23.13	6.9	-46.4	-77.00	89.00	1.00	2.00	-79.00	10.00	1.00	0.20
	10/20/15	167.30	-14.86	7.1	-126.7	-78.00	16.00	0.80	0.40	84.00	34.00	0.90	0.80
M31M	4/3/16	166.82	-14.35	6.9	-123.9	-74.00	29.00	0.80	0.80	-64.00	37.00	0.90	1.00
MAYO	10/20/15	167.30	-14.86	7.1	-125.9	-69.00	18.00	1.10	0.20	-62.00	7.00	1.20	0.20
	9/26/15	-71.32	-30.81	6.3	125.6	-8.00	31.00	1.00	1.00	-5.00	89.00	1.00	2.00
	9/21/15	-71.38	-31.73	6.6	126.1	89.00	23.00	0.70	0.70	-80.00	89.00	0.80	2.00
	5/22/15	163.22	-11.11	6.8	-120.8	-62.00	15.00	3.50	0.60	-62.00	10.00	3.50	0.80
	5/20/15	164.17	-10.88	6.8	-121.6	-51.00	16.00	2.10	0.80	-52.00	89.00	2.10	2.00
	5/7/15	154.56	-7.22	7.1	-111.4	-63.00	19.00	1.10	0.20	-64.00	14.00	1.10	0.20
	3/3/15	98.72	-0.78	6.1	-57.7	86.00	13.00	0.80	0.20	-85.00	19.00	0.90	0.40
	11/1/14	-177.76	-19.69	7.1	-141.0	-81.00	5.00	1.40	0.20	-76.00	4.00	1.50	0.20

continued on next page

continued from previous page

	Event Info					RC				SC			
Station	Date	Lon (°)	Lat (°)	Mag	Φ (°)	ϕ (°)	σ_ϕ	δt (s)	$\sigma_{\delta t}$	ϕ (°)	σ_ϕ	δt (s)	$\sigma_{\delta t}$
	10/9/14	-110.81	-32.11	7.0	158.7	-64.00	29.00	0.50	0.50	-73.00	37.00	0.50	0.70
	7/8/14	168.40	-17.69	6.2	-127.9	-83.00	24.00	1.10	0.50	-72.00	16.00	1.20	0.50
	5/4/14	178.24	-25.81	6.3	-139.3	-77.00	89.00	1.30	2.00	-79.00	89.00	1.30	2.00
	4/26/14	-174.71	-20.75	6.1	-144.0	-84.00	11.00	1.60	0.50	-80.00	19.00	1.70	1.10
	4/13/14	162.05	-11.46	7.4	-119.9	-81.00	35.00	0.60	0.90	-68.00	43.00	0.60	1.80
	4/12/14	155.24	-7.10	6.1	-111.9	-50.00	89.00	2.90	2.00	-48.00	60.00	2.90	1.50
MMPY	7/4/14	152.81	-6.23	6.5	-105.2	-52.00	15.00	0.40	0.20	-48.00	41.00	0.40	0.90
NOWN	4/7/15	-173.22	-15.17	6.3	-135.4	77.00	33.00	1.10	1.00	84.00	33.00	1.00	0.80
	12/7/14	154.46	-6.51	6.6	-102.7	27.00	19.00	0.90	0.40	26.00	24.00	0.90	0.40
	12/6/14	130.48	-6.11	6.0	-80.8	-40.00	89.00	2.00	2.00	-40.00	89.00	2.00	2.00
TGTN	10/20/15	167.30	-14.86	7.1	-119.2	-70.00	16.00	1.00	0.20	-84.00	14.00	1.10	0.30
	5/24/15	-175.96	-19.39	6.2	-135.7	81.00	26.00	0.90	0.50	84.00	29.00	0.90	0.60
	12/29/14	121.52	8.63	6.1	-68.1	80.00	18.00	1.20	0.70	81.00	41.00	1.20	1.70
	11/1/14	-177.76	-19.69	7.1	-134.2	-77.00	7.00	1.20	0.10	-88.00	11.00	1.20	0.20
	7/21/14	-178.40	-19.80	6.9	-133.7	-88.00	21.00	1.10	0.50	-77.00	25.00	1.20	0.70
	7/19/14	-174.45	-15.82	6.2	-135.8	-79.00	6.00	1.50	0.00	-81.00	5.00	1.40	0.20
	7/14/14	126.48	5.71	6.3	-73.8	61.00	25.00	0.60	0.40	62.00	35.00	0.60	0.60
	7/8/14	168.40	-17.69	6.2	-121.3	-71.00	28.00	0.60	0.50	-63.00	27.00	0.70	0.50
	7/3/14	-176.45	-30.46	6.3	-139.2	-82.00	25.00	1.00	0.50	-84.00	25.00	1.00	0.40
	5/4/14	179.09	-24.61	6.6	-133.3	-75.00	89.00	1.40	1.40	-76.00	40.00	1.40	1.40
WGLY	11/11/15	-72.01	-29.51	6.8	135.9	-15.00	18.00	1.30	0.50	-14.00	23.00	1.30	0.70

continued on next page

continued from previous page

	Event Info					RC				SC			
Station	Date	Lon (°)	Lat (°)	Mag	Φ (°)	ϕ (°)	σ_ϕ	δt (s)	$\sigma_{\delta t}$	ϕ (°)	σ_ϕ	δt (s)	$\sigma_{\delta t}$
	9/21/15	-71.38	-31.73	6.6	136.2	-10.00	34.00	0.70	0.70	3.00	35.00	0.70	0.60